

## Magnetoprobing of the discrete level spectrum of open quantum dots

J. P. Bird, R. Akis, and D. K. Ferry

*Center for Solid State Electronics Research and Department of Electrical Engineering, Arizona State University, Tempe, Arizona 85287-5706*

(Received 17 May 1999)

Through a detailed comparison of experiment and theory, we show that the features observed in the low temperature magnetoresistance of open quantum dots may be interpreted as arising from a magnetospectroscopy of their discrete density of states. At temperatures where ensemble averaging is only weakly effective, we find that the position and width of various peaks observed in this magnetoresistance may be associated with a resonance structure that is closely related to the density of states. This association can even be made in situations where the dot is strongly coupled to an external environment. [S0163-1829(99)05443-0]

### I. INTRODUCTION

Semiconductor quantum dots are submicron-sized electron cavities whose coupling to the external environment may be regulated by means of quantum point contact leads. With these leads configured so that current flow through the dot may only occur by tunneling, it is well established that transport measurements may be used to probe discrete electron states within the dot.<sup>1-4</sup> A more complicated issue, however, concerns the manner in which these states are modified when the dot is coupled to external reservoirs.<sup>5-9</sup> With the coupling provided by quantum point contacts, electrons are injected into the dot in a highly *collimated*<sup>10</sup> beam that couples selectively to preferred dot states.<sup>7-9</sup> This mode-matching process may be modulated by the application of a weak magnetic field, which sweeps the resonant dot states past the Fermi surface. At temperatures where this evolution can be thermally resolved, the magnetoresistance is thus expected to exhibit an oscillatory variation,<sup>11</sup> the details of which should provide information on the manner in which the dot spectrum is modified by the environmental coupling.<sup>12</sup>

In this paper, we describe the use of magnetotransport measurements to probe the discrete level spectrum of open quantum dots. At temperatures where ensemble averaging is effective ( $\geq 1$  K), the magneto-resistance of such devices is known to exhibit a pronounced peak at zero magnetic field,<sup>13-18</sup> whose lineshape has been argued to provide a probe of electron dynamics in the dot.<sup>19,20</sup> Here, however, our interest lies in the behavior observed at much lower temperatures, where ensemble averaging is ineffective and where experiments have shown that the zero-field peak is often obscured by reproducible fluctuations.<sup>21-25</sup> Through a detailed comparison of experiment and theory, we show that the magnetoresistance features observed in this regime may be interpreted as arising from a magnetospectroscopy of discrete states in the open dot. Specifically, we find that both the position and width of various magnetoresistance features are set by the underlying conductance resonance structure of the dot. A common feature of experiments performed in this regime is the observation of a zero-field peak in the magnetoresistance, whose amplitude varies nonmonotonically with gate voltage.<sup>15,17</sup> This characteristic is understood to result as

the gate voltage sweeps different resonant dot states past the Fermi surface at zero-magnetic field. Similar reasoning can also be used to account for the occurrence of pronounced resistance side-peaks at finite magnetic fields, which are another widely observed feature in the low-temperature regime.

The organization of this report is as follows. In the following section, we demonstrate the connection between the density of states and the conductance of open dots. In Sec. III, we present our experimental results and compare these with the findings of our numerical simulations. We conclude with a discussion of the implications of our findings in Sec. IV.

### II. CONDUCTANCE AND THE DENSITY OF STATES

The connection between the conductance of an open dot and its density of states is illustrated in Fig. 1. In Fig. 1(a), we show the computed energy spectrum of the isolated dot, which was obtained by solving a two-dimensional finite-difference Schrödinger equation with Dirichlet boundary conditions. In Fig. 1(b), we show the magnetoconductance contour of the dot in the case where current flow through the dot occurs by means of tunnel barriers that extend uniformly across its width. In Figs. 1(c) and 1(d), in contrast, we show the corresponding contours obtained when the point contact leads of the dot are opened to support one and four propagating modes, respectively. These conductance contours were computed using a lattice discretization of the Schrödinger equation, the details of which have been described elsewhere.<sup>7</sup> As one would expect for resonant tunneling through a double-barrier system, Fig. 1(b) shows a clear correlation between points of high conductance and the level spectrum of Fig. 1(a). An unexpected feature, however, is the nonuniform amplitude variation among the tunneling resonances, which indicates that, even with the environmental coupling provided by uniform tunnel barriers, the influence of this coupling is different for different dot states. A similar correlation between the conductance and the density of states is also found for the open dot, but is somewhat modified due to the fact that the external coupling is now provided by point contact leads [Figs. 1(c) and 1(d)]. Instead of the simple conductance peaks observed for the tunneling case [Fig. 1(b)], the resonances found with the leads present tend

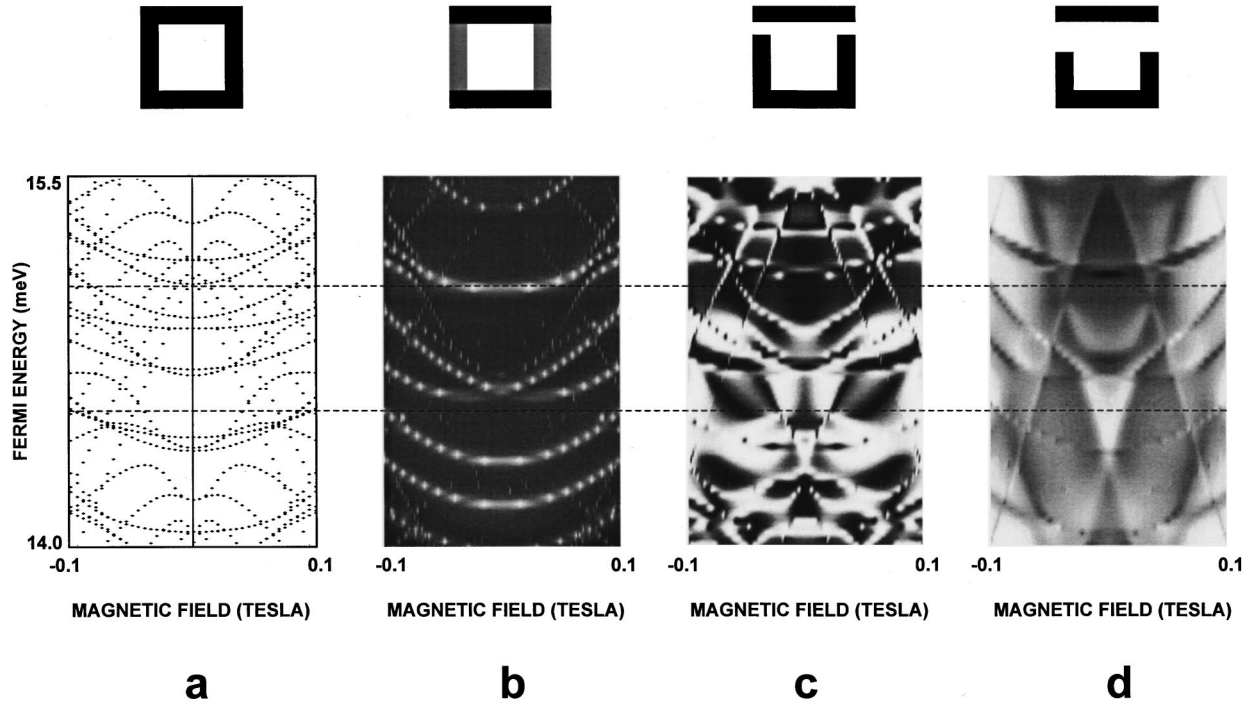


FIG. 1. (a) The computed energy levels of a  $0.3\text{-}\mu\text{m}$  hard-walled quantum dot of square geometry. (b) The tunneling spectrum for the same dot. (c) The conductance contour for the dot when its leads are opened to support one propagating mode. (d) The conductance contour for the dot when its leads are opened to support four propagating modes. In (b)–(d), conductance is plotted on a logarithmic scale and brighter regions correspond to points of higher conductance. All calculations were performed assuming a temperature of absolute zero.

to exhibit a Fano-line shape,<sup>26</sup> in which resonant transmission peaks are closely paired with resonant minima. Moreover, while the conductance of the isolated dot is strongly suppressed in situations where resonant tunneling is not possible, open dots exhibit more complicated behavior. To illustrate this, in Fig. 1 we have drawn dashed lines at two strategically chosen values of the Fermi energy. The upper line coincides with an energy for which the level spectrum is highly degenerate at zero field. In correspondence with this, the tunneling transport shows a resonant conductance peak [Fig. 1(b)], while in Fig. 1(d) the zero-field conductance is also seen to be high at this particular energy. In Fig. 1(c), however, the zero-field conductance actually shows a *minimum* at this Fermi energy. The second dashed line in Fig. 1 is positioned at an energy for which no states exist at zero-magnetic field, consistent with which tunneling through the isolated dot is strongly suppressed. The open dot with one mode in its leads also shows a local minimum at this energy, but this is now bounded by two resonant maxima. In the more strongly open dot, however, these maxima are seen to be broadened out sufficiently so that a region of high conductance is actually obtained [Fig. 1(d)].

The implication of the foregoing discussion is that transport measurements may be used as an experimental probe of the level spectrum of open dots. To interpret the results of such studies, however, we must recall that they are performed at nonzero temperatures, where energy averaging arises due to thermal smearing of reservoir states and electron dephasing in the dot. To simulate the effect of this averaging on the transport measurements, we adopt the following approach. We first account for thermal smearing and dephasing by introducing an effective temperature ( $T^*$ ), the choice of which is determined by appealing to the results of

experiment (see Sec. III below). At a given Fermi energy ( $E_F$ ), the energy averaged magneto-conductance may then be computed by solving the following integral numerically:

$$G_{av}(B, E_F) = \int G(E) \left[ -\frac{df(E - E_F)}{dE} \right] dE. \quad (1)$$

Since Eq. (1) shows that  $G_{av}$  is determined by convolving the resistance with the derivative of the Fermi-Dirac distribution function, in practice it is sufficient to integrate over an energy window, centered on the Fermi energy that is a few  $k_B T^*$  wide. At the very low temperatures of interest here, this window is thought to be sufficiently narrow to allow us to nonetheless resolve the passage of individual dot states past the Fermi surface.

### III. EXPERIMENTAL RESULTS AND NUMERICAL SIMULATIONS

#### A. Experimental approach

Both the fabrication and basic characterization of the quantum dots we study have been described in detail elsewhere.<sup>22</sup> These dots were defined on the surface of GaAs/Al<sub>x</sub>Ga<sub>1-x</sub>As heterojunction wafers, which were patterned into Hall bars to allow four-terminal resistance measurements to be made. At 4.2 K and after illumination with a red light-emitting diode, the carrier density and mobility of the wafer were found to be of order  $4.5 \times 10^{11} \text{ cm}^{-2}$  and  $400\,000 \text{ cm}^2/\text{Vs}$ , respectively. Magnetoresistance measurements were made at the base temperature of a dilution refrigerator, using standard lock-in detection and low-constant currents ( $\leq 1 \text{ nA}$ ) to avoid electron heating. While more than ten different dots have been studied to date, in this report we

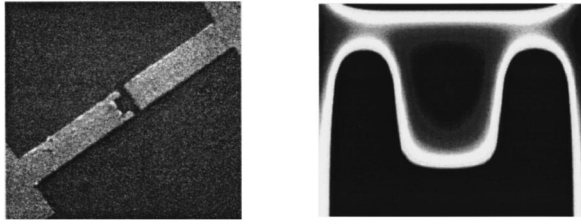


FIG. 2. Left: Scanning electron microscopy micrograph of the dot studied here. The central cavity has a lithographic dimension of  $0.4 \mu\text{m}$ . Right: Self-consistently computed potential profile for the same dot, in the case where the gate voltage is configured to allow two modes through the dot.

focus on the generic behavior exhibited by a lithographically square dot of side  $0.4 \mu\text{m}$  (Fig. 2). Due to the electrostatic fringing fields that develop around the gates, the actual size of the dot formed in the electron gas was somewhat smaller and was estimated to be of order  $0.25\text{--}0.3 \mu\text{m}$ , based on the observation of Aharonov-Bohm oscillations in the edge state regime.<sup>22</sup> These values in turn correspond to an average level spacing ( $\Delta$ ) in the dot ranging from  $1\text{--}1.3 \text{ K}$  ( $\Delta = 2\pi\hbar^2/m^*A$ , where  $A$  is the effective area of the dot).

### B. Basic experimental observations

In Fig. 3, we show the magnetoresistance of a split-gate dot and its variation with gate voltage. Similar to the behavior reported in other experiments,<sup>15,17</sup> a zero-field peak can be resolved in some of the traces, but the amplitude of this varies nonmonotonically with gate voltage. Indeed, in certain cases it is difficult to resolve any evidence for a peak, whatsoever. Another feature of the data is the emergence of pronounced *side peaks* at nonzero magnetic fields. As can be seen in Fig. 4, in which we plot selected traces from Fig. 3, these side peaks may rise to resistance values comparable to the height of the zero-field peak itself. From studies of dots with lithographic dimensions ranging from  $0.4$  to  $2 \mu\text{m}$ , both

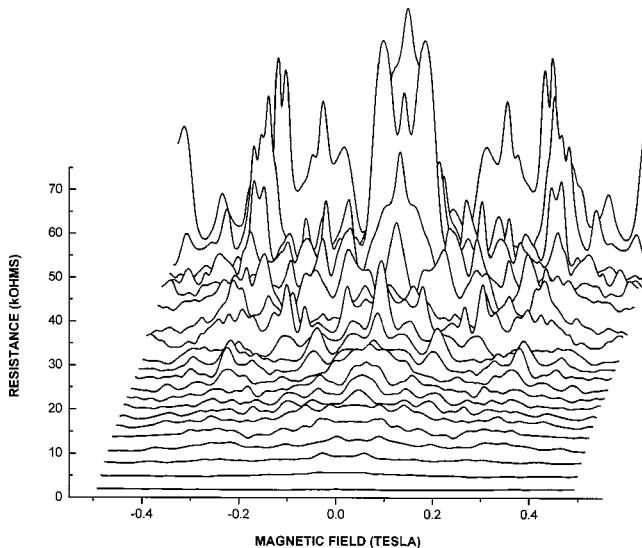


FIG. 3. The measured variation of the low temperature ( $0.01 \text{ K}$ ) magnetoresistance of the  $0.4\text{-}\mu\text{m}$  quantum dot with gate voltage. These magnetoresistance measurements were taken at 22 unequally spaced gate voltages ranging from  $-0.3610$  to  $-0.4335 \text{ V}$ .

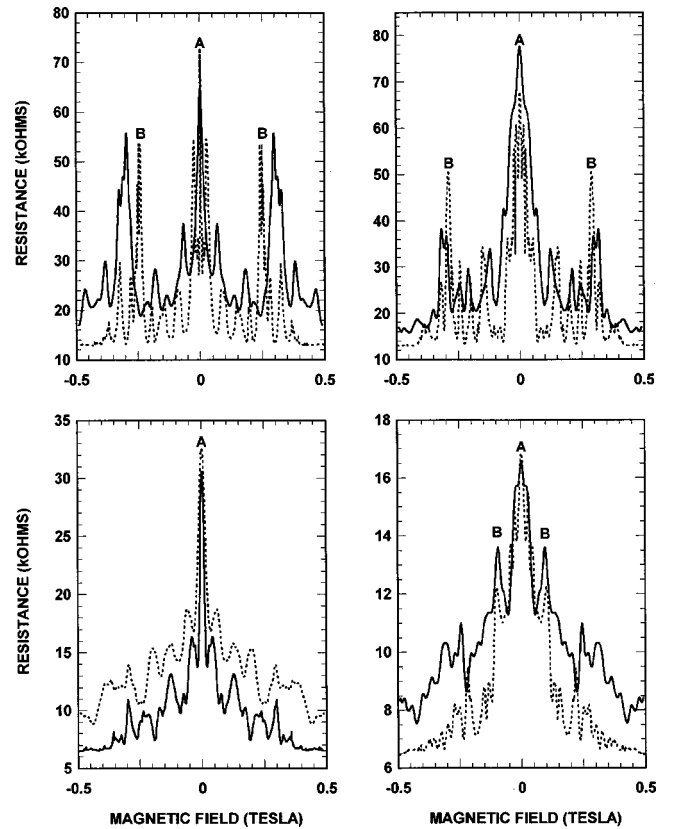


FIG. 4. In this figure, selected magneto-resistance curves from Fig. 3 are plotted (solid lines) and compared with the results of simulations (dashed lines). Upper left (experiment):  $V_g = -0.4295 \text{ V}$ . Upper left (simulation):  $V_g = -1.05 \text{ V}$ ,  $E_F = 15.75 \text{ meV}$ . Upper right (experiment):  $V_g = -0.4260 \text{ V}$ . Upper right (simulation):  $V_g = -1.05 \text{ V}$ ,  $E_F = 16.1 \text{ meV}$ . Lower left (experiment):  $V_g = -0.4000 \text{ V}$ . Lower left (simulation):  $V_g = -0.922 \text{ V}$ ,  $E_F = 15.1 \text{ meV}$ . Lower right (experiment):  $V_g = -0.3885 \text{ V}$ . Lower right (simulation):  $V_g = -0.922 \text{ V}$ ,  $E_F = 15.5 \text{ meV}$ . In these plots, the symbols *A* and *B* are used to denote the major features in the magnetoresistance (see text for further discussion).

the nonmonotonic evolution of the zero-field peak and the development of side peaks at finite fields are found to be characteristic features of the low-temperature magnetoresistance. As we shall discuss below, these distinct features are thought to result from magnetoprobings of the discrete density of states of the open dots.

### C. Comparison of experiment and simulations

Our numerical simulations begin by using a three-dimensional (3D) Poisson solver<sup>27</sup> to generate a self-consistent dot profile, using the known parameters of the semiconductor substrate and the lithographic dimensions of the gates. Using Eq. (1), the energy averaged magneto-conductance of the dot can be computed at a series of different Fermi energies. In the calculations presented here, an effective temperature of  $0.3 \text{ K}$  was assumed, which choice was motivated by the results of experiment. This suggests that the lowest temperature to which electrons cool in the dots is  $0.1 \text{ K}$  and that the phase breaking time ( $\tau_\phi$ ) is of



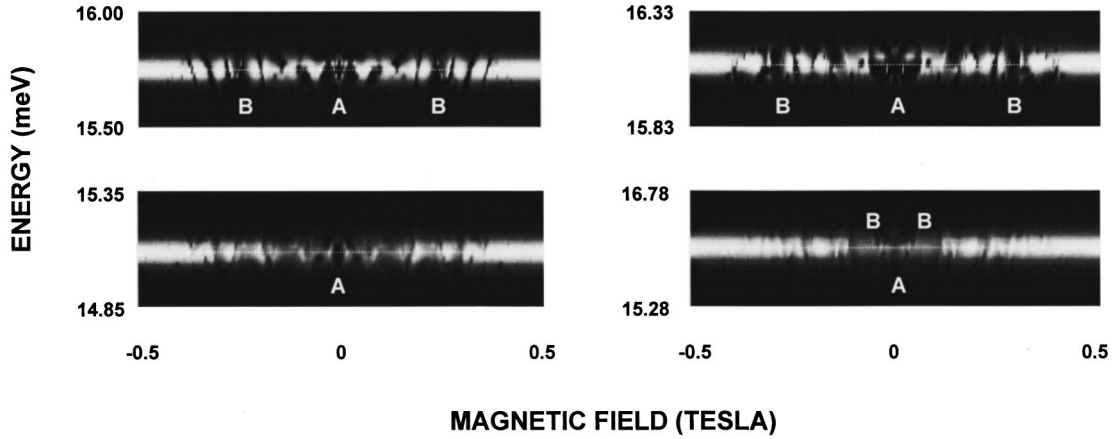


FIG. 5. Here, the conductance is convoluted with the derivative of the Fermi function and then plotted as a function of energy. The four figures correspond, in the same sequence, to the computed magnetoresistance plots shown in Fig. 4, while the symbols A and B denote the major magnetoresistance features seen in Fig. 4 (*see text for further discussion*).

order 100 ps.<sup>17,22,28–30</sup> Assuming dephasing to give rise to energy broadening of order  $\hbar/k_B\tau_\phi$  ( $\approx 0.1$  K), and noting that remnant disorder in the dot will further mix its discrete spectrum,<sup>31</sup> we believe this choice of effective temperature to be realistic.<sup>32</sup> As can be seen by comparing the experimental and theoretical curves in Fig. 4, our simulations are clearly successful in reproducing the main features of experiment. While we do not suggest that this agreement is perfect, we nonetheless believe it to be highly suggestive. In this regard, it is worth emphasizing that the experimental curves were obtained by varying *gate voltage*, which changes the size of the dot, and the width of its lead openings, in addition to modulating the electron density. In the simulations, in contrast, the *Fermi energy* is varied in a dot whose profile is kept *constant*. Consequently, we should not expect to obtain perfect agreement with the results of experiment. From a comparison in Fig. 4, however, it is clear that the simulations are able to account very well for the overall magnitude and magnetic field scales of the features seen in the experimental curves.

We have mentioned already that conductance measurements of open quantum dots can be thought of as providing a selective spectroscopy of their density of states (Fig. 1). The basic idea here is that a magnetic field or gate voltage may be used to sweep discrete dot states past the Fermi surface,<sup>11,12</sup> giving rise to an associated modulation of the conductance. The number of resonances that contribute to the conductance at any magnetic field is thus determined by the details of the density of states and the width of the window over which energy averaging is effective. At the low temperatures of interest here, the energy window is relatively narrow and the magnetoresistance should thus exhibit features associated with the movement of specific groups of dot resonances past the Fermi surface. Referring back to Fig. 1, it can be seen that the resonances tend to form boundaries between regions where the conductance is relatively slowly varying. In these flat regions, the conductance may be either high or low. When a low-conductance region exists at zero-magnetic field, a zero-field peak will arise whose width is set by the resonance lines that form the boundary for that region. The large side peaks noticed above occur for similar reasons. Conversely, one can obtain a zero-field minimum when the

Fermi energy lies in a region of relatively high conductance that is bounded by resonant minima. In the experiment here, the gate voltage is swept while the width of the energy window is (presumably) held constant. At each gate voltage, a unique portion of the density of states is therefore sampled, and it is this variation that is thought to give rise to the magnetoconductance modulation apparent in Fig. 3.

To illustrate these notions, in Fig. 5 we show the conductance contours that were used to calculate the magnetoresistance curves in Fig. 4. These contours were obtained by convoluting the magnetoconductance with the derivative of the Fermi function at a number of different energies. Brighter regions in the contours correspond to higher conductance and, at the low temperatures of interest here, only a narrow window contributes effectively to the energy average. An important feature of the contours is the series of bright and dark lines that pass through the Fermi level at different magnetic fields. In Fig. 1, we saw that these lines trace the evolution of the density of states as magnetic field and Fermi energy are varied. It is the presence of these lines that sets the position and widths of the major magnetoresistance peaks seen in experiment and theory. The width of the central peak found in the lower left panel of Fig. 4 (marked A), for example, is set by a pair of resonance lines that bound the local conductance minimum in the center of the lower-left panel of Fig. 5. Examining the other panels in Fig. 5, it is evident that similar features limit the width of the central peak in all other cases depicted in Fig. 4. Similarly, the side-peaks seen in the upper two plots of Fig. 4 result from the presence of a low conductance region that is bounded by resonances which cross the Fermi level near  $\pm 0.3$  T (Fig. 5, upper panels). Interestingly, the side-peaks are seen to be strongest in situations where the dot leads are configured to support just a few modes, a property that is apparent in both experiment and theory. Since the side peaks might easily be mistaken as arising from classical magneto-focusing, it is perhaps worth emphasizing that such an effect can be confidently ruled out here. Firstly, the magnetic field values at which the peaks occur do not seem to correspond to any obvious commensurability condition in the dot. Secondly, the peaks rapidly wash out with increasing temperature (not

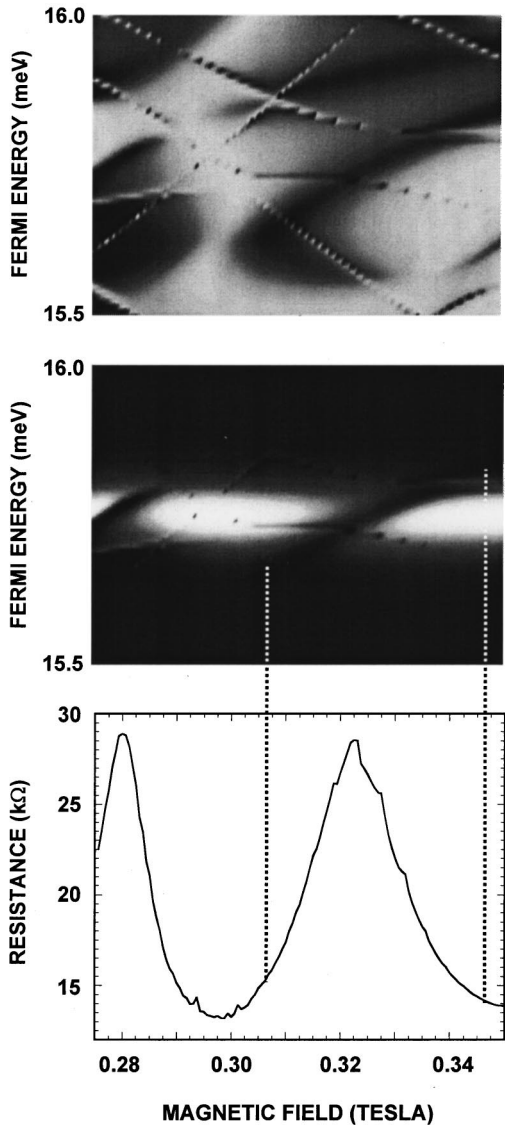


FIG. 6. Top: computed conductance contour of a  $0.4\text{-}\mu\text{m}$  dot at a gate voltage of  $V_g = -0.922\text{ V}$ . Middle: the contour obtained after convolving the conductance with the derivative of the Fermi function, assuming an effective temperature of  $T^* = 0.3\text{ K}$ . Bottom: the energy averaged magneto-conductance of the dot, computed from Eq. (1) assuming a Fermi energy of  $15.75\text{ meV}$  and an effective temperature of  $T^* = 0.3\text{ K}$ .

shown here), while focusing-related features are known to persist to very much higher temperatures.<sup>24,25,33,34</sup>

The influence of the Fermi surface crossings on the lineshape of the magnetoresistance is shown more clearly in Fig. 6. The upper panel of this figure shows the computed conductance contour for a particular dot. In the middle panel,

this contour is convoluted with the derivative of the Fermi function to show the range of energies that effectively contribute to the conductance. Here, we focus on the dark striation that passes through the Fermi surface over the magnetic-field range between  $0.3$  and  $0.35\text{ T}$ . This striation is thought to represent the passage of a broad resonance past the Fermi surface and it is easily seen that the magnetic-field range over which the crossing occurs determines the effective width of the resulting resistance peak.

#### IV. CONCLUDING REMARKS

Our results demonstrate how low temperature magnetotransport studies may be used as a spectroscopic probe of the discrete level spectrum in open quantum dots. Magnetoresistance features such as the zero-field peak, and also the pronounced side-peaks observed at nonzero magnetic fields, may be understood as arising from the Fermi-surface crossings of resonance lines, which, in turn, reflect the details of the density of states. An important feature that can be seen already in Fig. 1 is that not all states of the closed dot contribute effectively to transport through its open counterpart. This characteristic was also noted in a recent experimental study, in which conductance oscillations were induced in a dot at zero-magnetic field by sweeping the voltage applied to its defining gates.<sup>12</sup> The weighting of different closed-dot states in transport through the open dot is thought to be determined by a mode-matching process, involving the discrete states of the dot and the quantum-mechanical leads. Due to the quantization of transverse motion within these latter structures, electrons may only enter the dot by matching their transverse momentum component to one of the quantized values within the input lead. Electrons are therefore injected into the dot in a collimated beam that is only able to couple to those states whose momentum components it closely matches.<sup>7</sup> That is, opening the dot by means of quantum point contacts does not obscure its discrete level spectrum, but rather results in a subset of dot states being excited in transport.<sup>8,9</sup>

In conclusion, we have shown that features observed in the low-temperature magnetoresistance of open dots may be interpreted as arising from a magnetospectroscopy of their discrete level spectrum. The position and width of the various resistance peaks, found at a given Fermi energy, can be associated with an underlying resonance structure that is in turn closely related to the density of states of the dot. Such an association can even be made in the presence of level-broadening effects.

#### ACKNOWLEDGMENTS

This work was supported by RIKEN and the Office of Naval Research.

<sup>1</sup>P. L. McEuen, E. B. Foxman, U. Meirav, M. A. Kastner, Y. Meir, N. S. Wingreen, and S. J. Wind, *Phys. Rev. Lett.* **66**, 1926 (1991).

<sup>2</sup>R. C. Ashoori, H. L. Störmer, J. S. Weiner, L. N. Pfeiffer, S. J. Pearton, K. W. Baldwin, and K. W. West, *Phys. Rev. Lett.* **68**,

3088 (1992).

<sup>3</sup>A. T. Johnson, L. P. Kouwenhoven, W. de Wong, N. C. van der Vaart, C. J. P. M. Harmans, and C. T. Foxon, *Phys. Rev. Lett.* **69**, 1592 (1992).

<sup>4</sup>S. Tarucha, D. G. Austing, T. Honda, R. J. van der Hage, and L.

- P. Kouwenhoven, Phys. Rev. Lett. **77**, 3613 (1996).
- <sup>5</sup>J. Wang, Y. Wang, and H. Guo, Appl. Phys. Lett. **65**, 1793 (1994).
- <sup>6</sup>Y. Wang, N. Zhu, J. Wang, and H. Guo, Phys. Rev. B **53**, 16 408 (1996).
- <sup>7</sup>R. Akis, D. K. Ferry, and J. P. Bird, Phys. Rev. B **54**, 17 705 (1996).
- <sup>8</sup>I. V. Zozoulenko, R. Schuster, K. F. Berggren, and K. Ensslin, Phys. Rev. B **55**, R10 209 (1997).
- <sup>9</sup>I. V. Zozoulenko and K. F. Berggren, Phys. Rev. B **56**, 6931 (1997).
- <sup>10</sup>C. W. J. Beenakker and H. van Houten, Solid State Phys. **44**, 1 (1991).
- <sup>11</sup>M. Persson, J. Pettersson, B. von Sydow, P. E. Lindelof, A. Kristensen, and K. F. Berggren, Phys. Rev. B **52**, 8921 (1995).
- <sup>12</sup>J. P. Bird, R. Akis, D. Vasileska, J. Cooper, Y. Aoyagi, and T. Sugano, Phys. Rev. Lett. **82**, 4691 (1999). In this report, density of states oscillations are actually observed in the conductance on sweeping *gate voltage*, but the basic principle is similar to the magnetoprobings effect discussed here.
- <sup>13</sup>A. M. Chang, H. U. Baranger, L. N. Pfeiffer, and K. W. West, Phys. Rev. Lett. **73**, 2111 (1994).
- <sup>14</sup>J. P. Bird, D. M. Olatona, R. Newbury, R. P. Taylor, K. Ishibashi, M. Stopa, Y. Aoyagi, T. Sugano, and Y. Ochiai, Phys. Rev. B **52**, R14 336 (1995).
- <sup>15</sup>M. W. Keller, A. Mittal, J. W. Sleight, R. G. Wheeler, D. E. Prober, R. N. Sacks, and H. Shtrikmann, Phys. Rev. B **53**, R1693 (1996).
- <sup>16</sup>R. P. Taylor, R. Newbury, A. S. Sachrajda, Y. Feng, P. T. Coleridge, C. Dettmann, N. Zhu, H. Guo, A. Delage, P. J. Kelly, and Z. Wasilewski, Phys. Rev. Lett. **78**, 1952 (1997).
- <sup>17</sup>A. G. Huibers, M. Switkes, C. M. Marcus, K. Campman, and A. C. Gossard, Phys. Rev. Lett. **81**, 200 (1998).
- <sup>18</sup>Y. Lee, G. Faini, and D. Mailly, Phys. Rev. B **56**, 9805 (1997).
- <sup>19</sup>H. U. Baranger, R. A. Jalabert, and A. D. Stone, Phys. Rev. Lett. **70**, 3876 (1993). [Also, see R. A. Jalabert, H. U. Baranger, and A. D. Stone, *ibid.* **65**, 2442 (1990), for a discussion of the relation of quantum dot magnetotransport to the problem of quantum chaos.]
- <sup>20</sup>The interpretation of Ref. 19 has been disputed in a more recent study, in which the zero-field peak has been argued to reflect the influence of energy averaging on the level spectrum of the dot. [R. Akis, D. Vasileska, D. K. Ferry, and J. P. Bird, J. Phys.: Condens. Matter **11**, 4657 (1999); R. Akis, D. K. Ferry, J. P. Bird, and D. Vasileska, Phys. Rev. B **60**, 2680 (1999).]
- <sup>21</sup>C. M. Marcus, R. M. Westervelt, P. F. Hopkins, and A. C. Gosard, Phys. Rev. B **48**, 2460 (1993).
- <sup>22</sup>J. P. Bird, K. Ishibashi, Y. Aoyagi, T. Sugano, R. Akis, D. K. Ferry, D. P. Pivin, Jr., K. M. Connolly, R. P. Taylor, R. Newbury, D. M. Olatona, A. Micolich, R. Wirtz, Y. Ochiai, and Y. Okubo, Chaos Solitons Fractals **8**, 1299 (1997).
- <sup>23</sup>A. S. Sachrajda, R. Ketzmerick, C. Gould, Y. Feng, P. J. Kelly, A. Delage, and Z. Wasilewski, Phys. Rev. Lett. **80**, 1948 (1998).
- <sup>24</sup>L. Christensson, H. Linke, P. Omling, P. E. Lindelof, I. V. Zozoulenko, and K. F. Berggren, Phys. Rev. B **57**, 12 306 (1998).
- <sup>25</sup>P. Bøggild, A. Kristensen, H. Bruus, S. M. Reimann, and P. E. Lindelof, Phys. Rev. B **57**, 15 408 (1998).
- <sup>26</sup>Z. Shao, W. Porod, and C. S. Lent, Phys. Rev. B **49**, 7453 (1994).
- <sup>27</sup>D. Vasileska, M. N. Wybourne, S. M. Goodnick, and A. D. Gunther, Semicond. Sci. Technol. **13**, A37 (1998).
- <sup>28</sup>J. P. Bird, K. Ishibashi, D. K. Ferry, Y. Ochiai, Y. Aoyagi, and T. Sugano, Phys. Rev. B **51**, R18 037 (1995).
- <sup>29</sup>R. M. Clarke, I. H. Chan, C. M. Marcus, C. I. Duruöz, J. S. Harris, Jr., K. Campman, and A. C. Gossard, Phys. Rev. B **52**, 2656 (1995).
- <sup>30</sup>D. P. Pivin, Jr., A. Andresen, J. P. Bird, and D. K. Ferry, Phys. Rev. Lett. **82**, 4687 (1999).
- <sup>31</sup>A. Altland and Y. Gefen, Phys. Rev. B **51**, 10 671 (1995).
- <sup>32</sup>We have also performed simulations for an effective temperature of 0.2 K and find that this does *not* significantly modify the results presented here. In this regard, it appears that the order of magnitude, rather than the absolute value, of the effective temperature is crucial to reproducing the behavior found in experiment.
- <sup>33</sup>R. P. Taylor, A. S. Sachrajda, J. A. Adams, P. T. Coleridge, and P. Zawadzki, Phys. Rev. B **47**, 4458 (1993).
- <sup>34</sup>P. D. Ye and S. Tarucha, Phys. Rev. B **59**, 9794 (1999).